Desalination and Water Treatment
www.deswater.com

doi: 10.5004/dwt.2018.21980

108 (2018) 353–361
March

Synthesis of surface-functionalized ZnS nanoparticles and its potential application as methylene blue adsorbent

S. Daniel Devasangeeth[a], G.L. Balaji[a,*], R. Lakshmipathy[b,c,*]

[a]*Department of Chemistry, Thantai Hans Roever College, Perambalur, Tamil nadu, India,*
emails: sangeethchemistry@gmail.com (S.D. Devasangeeth), balajivinayaka84@gmail.com (G.L. Balaji)
[b]*Department of Chemistry, KCG College of Technology, Karapakkam, Chennai, Tamil nadu, India 600097*
[c]*Department of Chemistry, Hindustan Institute of Technology and Science, Padur, Chennai, India,*
email: lakshmipathy.vit@gmail.com

Received 17 August 2017; Accepted 1 February 2018

ABSTRACT

The study reports the use of surface modified ZnS nanoparticles as potential adsorbent for the removal of methylene blue (MB) from aqueous solution. The surface of the ZnS nanoparticles was modified with EDTA (E-ZnS) and watermelon rind extract (W-ZnS) and later characterized for its surface properties. The size of surface modified ZnS nanoparticles was found to be spherical shape with an average size of 12 and 10 nm, respectively, for W-ZnS and E-ZnS NPs. As an application, the ZnS nanoparticles were investigated for the sequestration of MB from aqueous solution. Batch adsorption studies were employed to optimize the experimental conditions aiming MB removal. Batch parameters such as pH, contact time, adsorbent dose and initial adsorbate concentration were optimized. Isotherms and kinetic models were applied to study the mechanism of adsorption process. The process is found to be thermodynamically feasible and spontaneous in nature. The results suggest that the surface modification of ZnS nanoparticles enhanced the MB uptake capacity.

Keywords: ZnS nanoparticles; EDTA; Surface modification; Adsorption; Watermelon rind

1. Introduction

The increasing population and demand for industrial products have led to serious contamination of the environment. The persistence of contaminants especially in the water streams has badly affected the biotic and abiotic components of the ecosystem. There is an increasing concern on elimination of contaminants from industrial wastewater before it reaches the water streams. Various treatment techniques such as oxidation, ion exchange, reverse osmosis, electrochemical treatment, precipitation, adsorption, filtration, etc., are in practice for the removal of contaminants from wastewater [1]. In spite of all the techniques, adsorption is found to be superior and most economic technique for the treatment process [2]. Various adsorbents such as activated carbon [3], zeolites [4], agricultural wastes [5,6], ionic liquids [7] and nano materials [8] are investigated and reported in literature.

Among the adsorbents, nanosorbents are classified as promising adsorbent due to its high efficiency and easy separation process. The high efficiency exhibited is due to the high surface area and high activities caused by size quantization effect [9]. Hua et al. [10] reported an informative review on use of various nano/nano metal oxide sorbents for treatment of heavy metal ions from wastewater. A detailed literature review suggested that much of the work has been investigated on nano metal oxides for the heavy metal ion and dye treatment from wastewater. The reports on use of nano metal sulfides as adsorbents is very minimal and yet to be explored.

* Corresponding author.

Semiconductor nanoparticles (NPs) in the size ranging from 1 to 10 nm have received much interest because of their unique properties. Especially, the II–VI semiconductors having wide band gaps and studied for their extensive use in optoelectronic devices [11]. Among II–VI semiconductor NPs, zinc sulphide (ZnS) was considered to be an important material which has a wide band gap 3.5 eV for cubic phase at room temperature. The ZnS NPs have high catalytic functions and are effectively used as photocatalyst for the degradation of methylene blue (MB) dye [12,13]. The ZnS NPs are investigated as photocatalytic agents, their applications as adsorbent in the removal of adsorbates are yet to be investigated. Recently, Ni-doped ZnS NPs loaded onto activated carbon was investigated as potential adsorbent for the removal of Congo red dye from aqueous solution [14].

According to Lakshmipathy et al. [15], the acid group from the citrulline binds onto the surface of the ZnS NPs and thus the amino groups are freely available at the surface. The presence of amino group on the surface will facilitate binding of anions rather than cations. The study also reported that the presence of functional groups on the surface of ZnS NPs enhanced the photocatalytic property by adsorbing the target analyte. Though the degradation was successfully achieved, the water still contains degraded analytes whose toxicity or effects are not validated or unknown. Further, the degradation mechanism takes place by adsorption of MB ions onto the surface of the ZnS NPs and catalytically degraded upon receipt of UV light. Since adsorption is powerful technique which delivers complete elimination of contaminants, the use of ZnS NPs as adsorbent shall be highly significant for the removal of MB ions from aqueous solution. In the present study, the synthesized ZnS nanoparticles (ZnS NPs) by adding watermelon rind (WR) extract as capping agent were investigated as an adsorbent for the complete removal of MB from aqueous solution. The surface of the ZnS NPs is reported to be bound by citrulline, an amino acid found abundantly in WR [15]. In order to make the ZnS NPs as cations sequester and most efficient adsorbent, the surface must be modified with acidic and hydroxyl groups. Thus, the ZnS NPs surface was functionalized with EDTA and characterized for its morphology. As an application, the surface functionalized ZnS NPs were investigated as potential nanosorbent for the removal of MB from aqueous solution.

2. Materials and methods

2.1. Materials

The analytical grade zinc acetate and sodium sulphide was procured from SD Fine-Chem Ltd., India. The analytical grade EDTA and MB was procured from Merck, India, with 99.9% purity. Deionized water was used for making up all reagents and test solutions.

2.2. Synthesis of EDTA-functionalized ZnS NPs

The ZnS NPs were synthesized according to the procedure reported in the literature [15]. A 1:1 molar ratio of zinc acetate and sodium sulfide (Na_2S) solutions at room temperature was mixed and spontaneously a white precipitate of ZnS was observed. To this ZnS colloid, WR extract was added, followed by vigorous stirring using a magnetic stirrer for 90 min at room temperature then centrifugation at 10,000 rpm for 10 min. The product obtained after discarding the supernatant was washed with deionized water for several times in order to remove any impurities present on it. The water washed product was dried in oven at 100°C for 1 h and named as WR-capped ZnS nanoparticles (W-ZnS NPs). The procedure adopted for synthesis of EDTA-capped ZnS NPs is very similar to the W-ZnS NPs. The 1:0.5 of zinc acetate and EDTA was dissolved in deionized water and to this solution, Na_2S solution was added drop by drop with constant stirring (Fig. 1). Formation of white color precipitate ZnS was observed during the addition of Na_2S and continued till no more precipitate formation was observed. The mixture was stirred well with the help of a magnetic stirrer at 100 rpm at 60°C for 12 h. After stirring, the solid ZnS NPs were separated by centrifugation process. The suspension was centrifuged at 10,000 rpm for 10 min at 3°C. The supernatant solution was stored for further analysis and the solid ZnS NPs obtained were dried in oven at 80°C for 5 h. The obtained solid was named as E-ZnS NPs and subjected for characterization.

2.3. Characterization techniques

The functionalization of EDTA onto ZnS NPs was confirmed by Fourier transform infrared (FTIR) analysis (Avatar 330, Thermo Nicolet). The samples were scanned from 4,000 to 400 cm^{-1} for 32 times in transmittance mode. Transmission electron microscope (TEM; JEM-2100F) was employed to know the size and shape of the synthesized ZnS NPs. Powder XRD analysis of the synthesized ZnS NPs was carried out using a D8 Advance diffractometer, Bruker, Germany, (with Cu Ka radiation, k = 1.54 Å) equipped with a Lynx eye detector and b-Ni filter, scanning in the 2 h range from 10° to 80° at 0.02° min^{-1}.

2.4. Batch adsorption studies

Batch adsorption studies were carried out for the removal of MB from aqueous solution by W-ZnS and E-ZnS

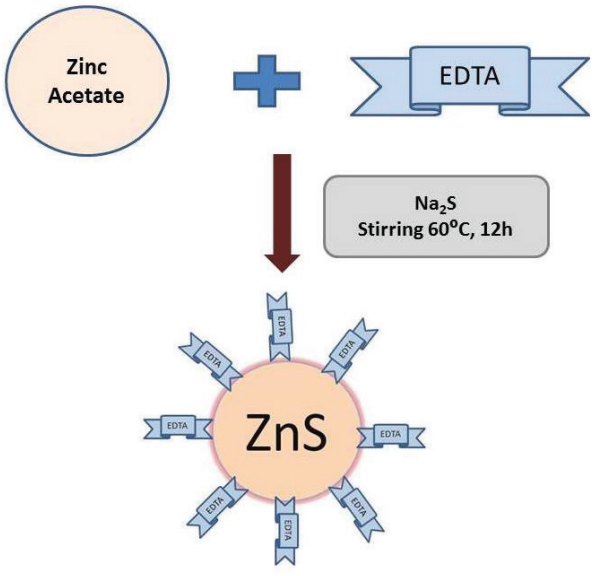

Fig. 1. Synthesis of EDTA-functionalized ZnS nanoparticles.

NPs. Batch parameters such as pH, contact time, adsorbent dose, initial adsorbate concentration and temperature were optimized. The batch studies were carried out by adding appropriate adsorbents to 20 mL of prefixed concentration of MB solution for optimizing the parameters except for initial adsorbate concentration. The suspension was agitated at 150 rpm in a temperature-controlled orbital shaker. The suspension was separated by centrifugation process and the residual concentration of MB present in the solution was determined by UV-visible spectrometer. The concentration of MB in the solution was measured at λ_{max} 665 nm with reference to the known standard solution. All the experiments were conducted for triplicate and the mean values are represented here. The error was found to be less than 3%. The percentage removal and loading capacity of the process was determined by the following equations:

$$\%\ \text{Removal of MB} = q_e = (C_0 - C_1)\frac{V}{M} \quad (1)$$

$$\text{Loading capacity} = \%\text{Removal} = \frac{(C_0 - C_1)}{C_0} \times 100 \quad (2)$$

where C_0 is the initial adsorbate concentration and C_1 is the final adsorbate concentration. V is the volume and M is the mass of the adsorbent.

3. Results and discussion

3.1. Characterization of W-ZnS and E-ZnS NPs

3.1.1. FTIR

The FTIR analysis was carried out in order to confirm the binding of EDTA onto ZnS NPs. The FTIR spectra of ZnS, W-ZnS and E-ZnS nanoparticles are represented in Figs. 2 (a) & (b) and Fig. S1. The FTIR spectra of WR-mediated ZnS NPs show absorption peaks at 3,441 cm^{-1} correspond to O–H stretching of acidic part of amino acids and the dual bands one at 3,419 cm^{-1} corresponds to N–H stretching and the a shoulder peak at 3,200 cm^{-1} corresponds to an overtone of N–H bending vibrations of 1° amines present in the amino acid of the extract. The peaks at 2,926 and 2,854 cm^{-1} are attributed to C–H stretching. The strong absorption peaks at 1,631 cm^{-1} corresponds to C–O stretching and the band at 1,568 cm^{-1} corresponds to N–H bending. C–C stretching was observed at 1,402 cm^{-1}, the absorption peaks around 563 cm^{-1} correspond to Zn–S metal bond stretching. From the above analysis, it is clear that bio-molecular capping on the ZnS NPs especially the binding of major component of citrulline in WR extract. The FTIR spectra of EDTA-capped ZnS NPs exhibit absorption band at 3,388 cm^{-1} corresponding to O–H stretching due to moisture content present in the sample. The intense peaks at 1,581 cm^{-1} correspond to the asymmetrical stretching of COO^- groups and band at 1,409 cm^{-1} correspond to C–C stretching vibrations. The band at 1,325 cm^{-1} is attributed to C–CO_2 groups of EDTA. The peak at 1,109 cm^{-1} corresponds to C–N groups. The other weak bands attribute to stretching and bending vibrations of C–N–C and C–O–O groups. These observations confirm the binding of EDTA on the surface of ZnS NPs.

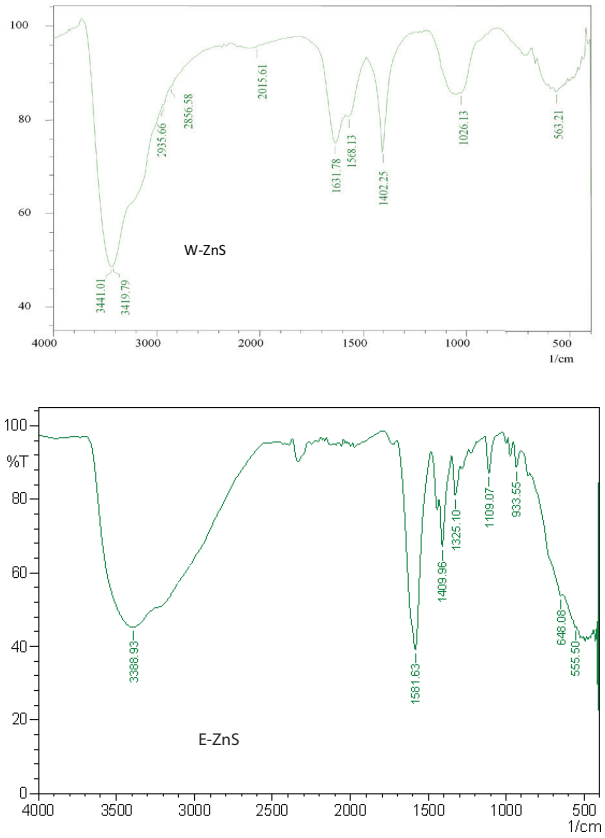

Fig. 2. FTIR spectra of W-ZnS and E-ZnS nanoparticles.

3.1.2. TEM

The TEM analysis was carried out to know the shape and size of the synthesized ZnS NPs. The TEM image of E-ZnS NPs is represented in Fig. 3. The size of the E-ZnS NPs is found to be around 10 nm; however, the shape of the NPs is found to be irregular in shape and found to have agglomeration. The TEM micrograph suggests that the functionalization of EDTA onto ZnS did not avoid agglomeration. This is due to binding of freely available COO^- groups from EDTA onto other adjacent ZnS NPs. In case of W-ZnS NPs, the size and shape of the NPs was found to be approximately 12 nm with spherical in shape [15]. The size distribution of W-ZnS, E-ZnS and ZnS NPs is represented in Fig. S3. It can be observed that the size distribution of ZnS is wide and no control of size due to absence of capping/stabilizing agents. In case of W-ZnS and E-ZnS, the size distribution range is less compared with unmodified ZnS. This is due to the factor that the presence of capping/stabilizing agents from WR extract and EDTA restricted the size growth of ZnS NPs.

3.1.3. XRD

The XRD analysis was carried out to determine the crystalline nature of the synthesized W-ZnS and E-ZnS NPs. The XRD patterns of W-ZnS and E-ZnS NPs are represented in Fig. 4. The diffraction peaks of W-ZnS NPs at 28.65°, 33.15°, 47.56°, 56.44°, 60.67° and 76.99° correspond to (111), (200), (220), (311), (400) and (331) planes of cubic ZnS (Fig. 4(a)).

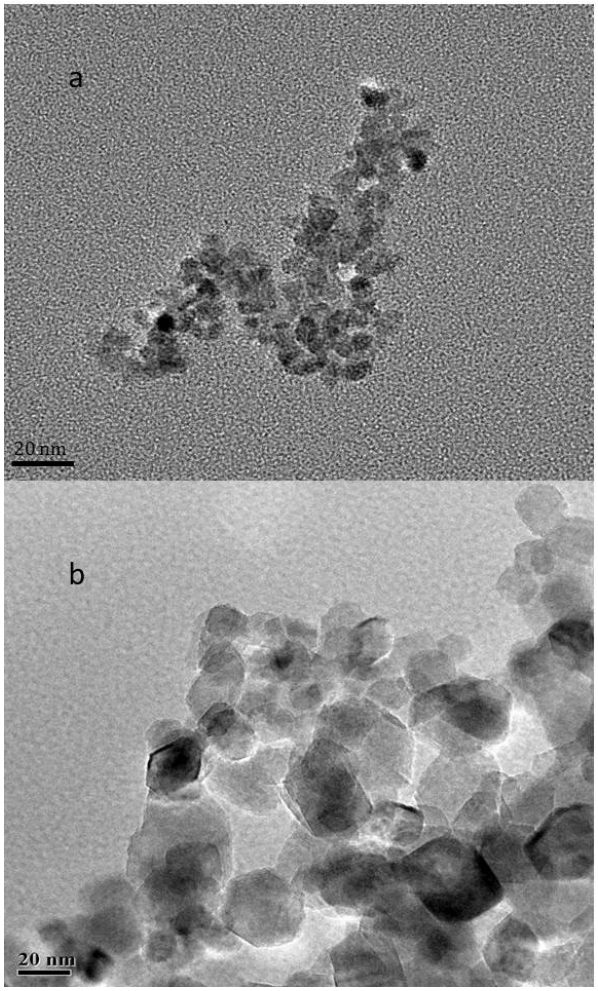

Fig. 3. TEM micrograph of E-ZnS nanoparticles.

The typical broadening of the peaks was observed, depicting that the synthesized ZnS NPs are small in size. The diffraction peaks of E-ZnS were also similar to that of W-ZnS NPs (Fig. 4(b)). The diffraction peaks of W-ZnS and E-ZnS NPs are found to be similar to that of unmodified ZnS (Fig. S2). These observations suggest that the functionalization of ZnS with WR extract and EDTA has not resulted in any phase change.

3.2. Batch adsorption studies

3.2.1. Effect of pH

The solution pH is an important parameter which must be optimized while performing adsorption studies. The presence of H^+ ion concentration in the solution will always exhibit competition to the target analytes for the adsorption sites. In view of the above factor, a study was executed to optimize the pH by varying the solution pH from 2 to 10 (Fig. 5). It was observed that with increase in pH of the solution, the removal efficiency increased and found maximum at pH 8 for W-ZnS NPs (Fig. 5). Similar trend was observed for EDTA-functionalized ZnS NPs; however, the maximum removal efficiency was found at pH 8 and observed to be saturated till pH 10. The increasing trend observed in both the

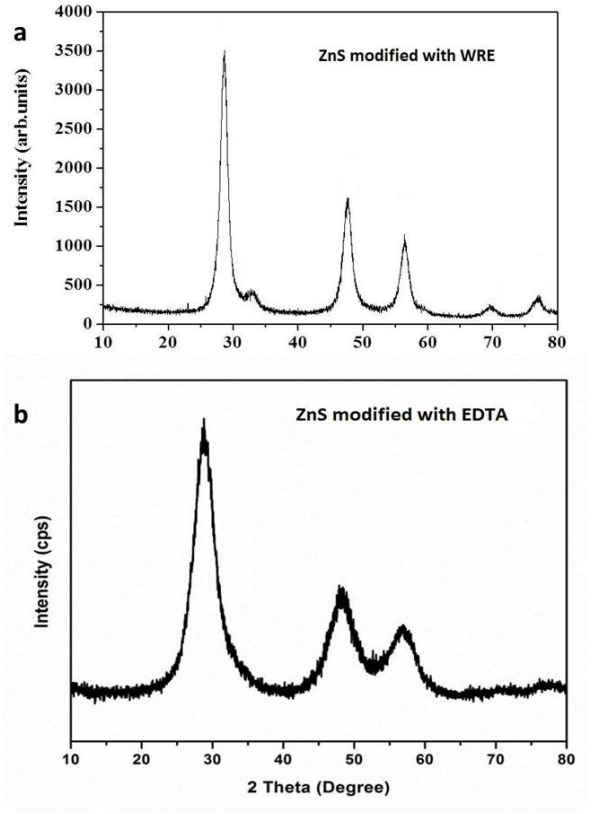

Fig. 4. XRD patterns of (a) W-ZnS and (b) E-ZnS nanoparticles.

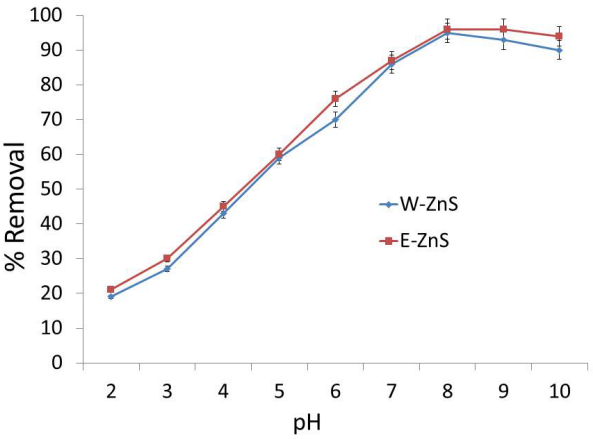

Fig. 5. Effect of pH on the removal of MB from aqueous solution (time 30 min, dose 1.5 g L^{-1}, MB concentration 50 mg L^{-1}).

cases is due to the decrease of H^+ ions concentration with the increasing pH thus minimizing the competitive adsorption for active sites. Further optimization studies were carried out at pH 8 for W-ZnS and E-ZnS NPs.

3.2.2. Effect of adsorbent dose

The adsorbent dose plays a vital role in adsorption studies which decides the cost of the treatment process [16]. In order to optimize the adsorbent dose, the dose of the W-ZnS and E-ZnS NPs was varied from 0.5 to 5 g L^{-1} and

the results are represented in Fig. 6. The removal efficiency of MB increased with increasing adsorbent dose and found to be saturated at 1.5 and 1 g L^{-1}, respectively, for W-ZnS and E-ZnS NPs. The increasing trend observed is due to the availability of more number of active sites with increasing adsorbent dose [17]. The efficiency is found to be saturated beyond 1 g L^{-1} due to agglomeration of adsorbents thus decreasing or blocking the active sites. The removal efficiency of E-ZnS NPs is found to be much higher and saturation point was reached earlier compared with W-ZnS NPs. The difference observed is due to presence of EDTA groups on the surface of the ZnS NPs enabling faster and easier binding process. Thus 1.5 and 1 g L^{-1} were fixed as adsorbent dose for further experiments.

3.3. Kinetics of adsorption

The kinetic experiments were performed very similar to the equilibrium experiments by varying the contact time and collecting the samples at preset time intervals. The experimental data obtained were analyzed with two well-known kinetic models such as pseudo-first order and pseudo-second order kinetic models.

The pseudo-first order rate equation of Lagergren is represented as follows:

$$\ln(q_e - q_t) = \ln q_e - k_1 t \tag{3}$$

where q_e is the amount of MB ion adsorbed at equilibrium (mg g^{-1}), q_t is the amount of MB ion adsorbed at time t and k_1 is the first-order reaction rate constant. A straight line of $\ln(q_e - q_t)$ vs. t suggests the applicability of this kinetic model and values of k_1 and q_e were determined from the plot.

Based on the sorption equilibrium capacity pseudo-second order equation can be expressed as:

$$\frac{t}{q_t} = \frac{1}{k_2 q_e^2} + \frac{t}{q_e} \tag{4}$$

where k_2 (g mg^{-1} min^{-1}) is the rate constant of pseudo-second order adsorption. The values of k_2 and q_e can be calculated from the plot of t/q_t vs. t.

The correlation coefficients and respective constants obtained for the kinetic models are summarized in Table 1. The correlation coefficients obtained for pseudo-first order is found to be low suggesting that pseudo-first order model is not applicable to the present process. The failure of the model is further supported by the theoretical q_e values which are not close enough to the experimental q_e values. The pseudo-second order kinetic model was found to fit well to the experimental data. The correlation coefficients were found to be close to 1 and further the theoretical q_e values were close to the experimental q_e values. These observations suggest that the removal of MB by W-ZnS and E-ZnS NPs follows pseudo-second order kinetics and the process controlling the rate-limiting step is chemical sorption involving valence forces through sharing or exchanging of electrons between sorbate and sorbent [18].

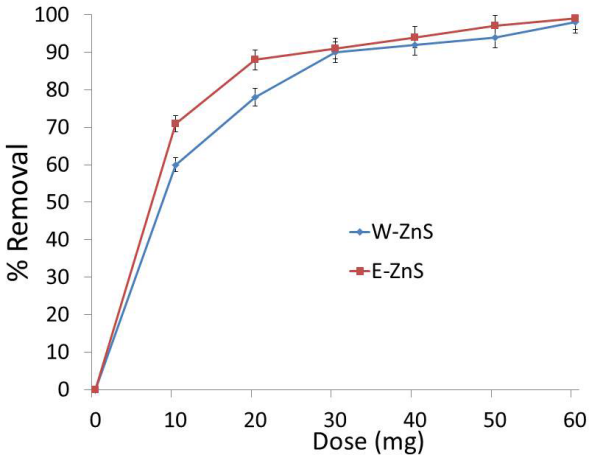

Fig. 6. Effect of dose on the removal of MB from aqueous solution (time 30 min, pH 8, MB concentration 50 mg L^{-1}).

3.4. Adsorption isotherms

The loading capacity of adsorbent is a prime criterion for selection of adsorbents for real-time treatment process. In order to evaluate the loading capacity of W-ZnS and E-ZnS NPs, at equilibrium, the initial concentration of the MB solution was varied from 50 to 300 mg L^{-1}. It was observed that with increase in initial concentration, the loading capacity increased and reached a maximum of 178.7 and 388.1 mg L^{-1}, respectively, for W-ZnS and E-ZnS NPs. The loading capacity of W-ZnS and E-ZnS NPs is found to be higher than many other adsorbents reported in literature and few of the loading capacities of adsorbents are summarized and compared in Table 2. The higher removal efficiency exhibited by E-ZnS NPs is due to presence of the acidic functional groups from EDTA on the surface enabling easier binding of MB. In case of citrulline-capped ZnS NPs, the surface exhibits amino groups which do not facilitate the binding of cations. The equilibrium data obtained were used for understanding the relationship between the concentration of adsorbate ions at equilibrium (C_e) and loading capacity (q_e). The relationship

Table 1
Kinetic constants derived for the plot of pseudo-first order and pseudo-second order models for the removal of MB from aqueous solution (pH = 7, MB concentration = 50 mg L^{-1} and dose-0.5 g L^{-1})

System	Pseudo-first order			Pseudo-second order		
	k_1 (min^{-1})	q_e (mg g^{-1})	R^2	k_2 (g mg^{-1} min^{-1})	q_e (mg g^{-1})	R^2
ZnS	0.019	14.8	0.856	0.067	58.4	0.999
E-ZnS	0.023	17.7	0.913	0.043	89.7	0.999

can be better understood by applying isotherm models such as Freundlich and Langmuir isotherms.

Freundlich isotherm is an empirical equation that is based on the sorption of an adsorbate on a heterogeneous surface of an adsorbent. The linear form of Freundlich isotherm is given as:

$$\log q_e = \log K_f + \frac{1}{n}\log C_e \quad (5)$$

where K_f and n are Freundlich constants which indicate the adsorption capacity and intensity, respectively. If Eq. (3) applies, a plot of log q_e vs. log C_e will give a straight line.

The Langmuir isotherm assumes monolayer adsorption process and linear form of Langmuir isotherm after rearrangement is given as:

$$\frac{C_e}{q_e} = \frac{1}{bV_m} + \frac{C_e}{V_m} \quad (6)$$

where C_e is the concentration of MB ions at equilibrium (mg L^{-1}), q_e is the amount of adsorbate adsorbed per unit mass of adsorbent (mg g^{-1}), V_m is the amount of adsorbate at complete monolayer coverage (mg g^{-1}) and b is a constant that relates to the heat of adsorption (L mg^{-1}). If the adsorption follows Langmuir isotherm then a plot of C_e/q_e vs. C_e should be a straight line with slope $1/V_m$ and intercept $1/bV_m$.

Table 2
Loading capacities of various adsorbents reported in literature

Adsorbent	Loading capacity (q_e) mg g^{-1}	Reference
ZnS:Cu-NP-AC	106.9	[19]
Ag NPs-AC	71.4	[20]
Pd NPs-AC	75.4	[20]
Graphene oxide calcium alginate composites	181.8	[21]
ZnS-NP-AC	100	[22]
Fe_3O_4/SiO_2 core/shell	111.1	[23]
Banana peel	20.8	[24]
Algerian kaolin	52.7	[25]
Pyrophyllite	4.2	[26]
W-ZnS	178.7	This study
E-ZnS	388.1	This study

The correlation coefficients and respective constants obtained for Freundlich and Langmuir isotherm are summarized in Table 3. The plots obtained for Freundlich isotherm are not linear (figure not shown) and correlation coefficients obtained are low, suggesting that Freundlich isotherm is not applicable to the present process. The plots of Langmuir isotherm for the obtained data are found to be linear (Fig. 7) and the correlation coefficients are also close to 1, suggesting the better fit of the model. The better fit is further supported by theoretical monolayer coverage (V_M) derived from plots of Langmuir isotherm are close to the calculated experimental values. The results suggest that the adsorption of MB onto W-ZnS and E-ZnS NPs is monolayer adsorption process.

3.5. Thermodynamics of adsorption

The removal of MB by W-ZnS and E-ZnS NPs was investigated at three different temperatures to understand the nature of the process. The thermodynamic parameters such as free energy change (ΔG°), enthalpy (ΔH°) and entropy (ΔS°) are derived from the experimental data and used for understanding the nature of adsorption process.

Thermodynamic parameters can be evaluated from the following equations:

$$K_D = \frac{q_e}{C_e} \quad (7)$$

$$\Delta G° = -RT\ln K_D \quad (8)$$

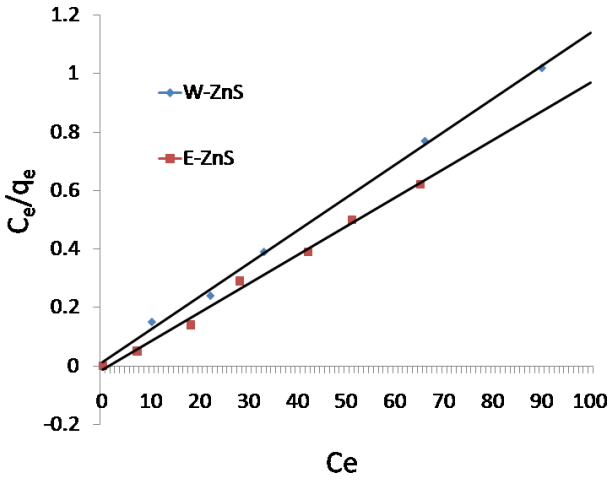

Fig. 7. Plots of Langmuir isotherm for the removal of MB by W-ZnS and E-ZnS NPs from aqueous solution.

Table 3
Parameters of Freundlich and Langmuir isotherm models for the removal of MB from aqueous solution (time = 30 min, temperature = 303 K, pH 7 and dose = 0.5 g L^{-1})

System	Freundlich isotherm			Langmuir isotherm		
	K_f	$1/n$	R^2	V_m (mg g^{-1})	b (L mg^{-1})	R^2
ZnS	9.07	0.033	0.901	177.2	0.034	0.989
E-ZnS	8.69	0.037	0.893	391.6	0.029	0.992

Table 4
Thermodynamic parameters derived for the removal of MB from aqueous solution (time = 30 min, MB concentration = 50 mg L^{-1}, pH 7 and dose-0.5 g L^{-1})

Adsorbent	Temperature (K)	Loading capacity (mg g^{-1})	$\Delta G°$ (kJ mol^{-1})	$\Delta H°$ (kJ mol^{-1})	$\Delta S°$ (J mol^{-1} K^{-1})
W-ZnS	303	58.4	–6.79	–6.14	412
	313	57.1	–5.96		
	323	54.5	–5.11		
E-ZnS	303	89.7	–9.63	–8.94	651
	313	88.3	–8.74		
	323	86.8	–7.38		

$$\Delta G° = \Delta H° - T\Delta S° \quad (9)$$

$$\ln K_D = \frac{\Delta S°}{R} - \frac{\Delta H°}{RT} \quad (10)$$

where K_D is the equilibrium constant, q_e is the amount of MB adsorbed at the surface of the adsorbent, C_e is the equilibrium concentration in solution (mg L^{-1}), R is the gas constant (8.314 J mol^{-1} K^{-1}), T is the temperature (K). The enthalpy ($\Delta H°$) and entropy ($\Delta S°$) of adsorption were estimated from the slope and intercept of the plot ln K_D vs. $1/T$, respectively.

The loading capacity of the adsorbents found to decrease with increase in temperature from 303 to 323 K. The decrease in loading capacities is due to weakening of the adsorption sites at higher temperatures. The thermodynamic parameters derived from the plots are summarized in Table 4. It is observed from Table 4 that the free energy values obtained for both the adsorbents are negative suggesting that the process is spontaneous in nature. However, the negative values found to decrease with increase in temperature suggesting that the spontaneity decreases with increase in temperature. The enthalpy ($\Delta H°$) values are found to be negative suggesting that the process is exothermic in nature and positive entropy ($\Delta S°$) values suggest that the increase in randomness of the MB ions at the adsorbent surface.

3.6. Desorption studies

The process of regeneration of the adsorbent and recovery of adsorbate are very important for selection of adsorbents in real-time industrial process. In view of the above, desorption of adsorbed MB ions from ZnS and E-ZnS NPs was investigated with various desorbing agents such as HCl, NaOH, H_2O and CH_3COOH. The experiments were carried by adding 0.1 g of MB-loaded W-ZnS in 20 mL of desorbing agents and agitated for 30 min at 303 K in a temperature-controlled orbital shaker. After the prescribed time interval, the suspension was separated by centrifugation process and the resultant supernatant solution was subjected to UV-visible spectrophotometer to determine the concentration of MB in the desorbed solution. Similar experiment was carried out for MB-loaded E-ZnS NPs. The average results of two replicates are represented in Fig. 8. It was observed that acetic acid showed higher desorption efficiency compared with other investigated desorbing agents followed by HCl, NaOH and H_2O. Further, the regenerated adsorbents were used for next sorption cycles. It was observed that the removal efficiency of E-ZnS NPs started decreasing after third cycle compared with W-ZnS NPs. The decrease in efficiency might be due to weakening of adsorption sites and leaching of EDTA from the surface of ZnS NPs.

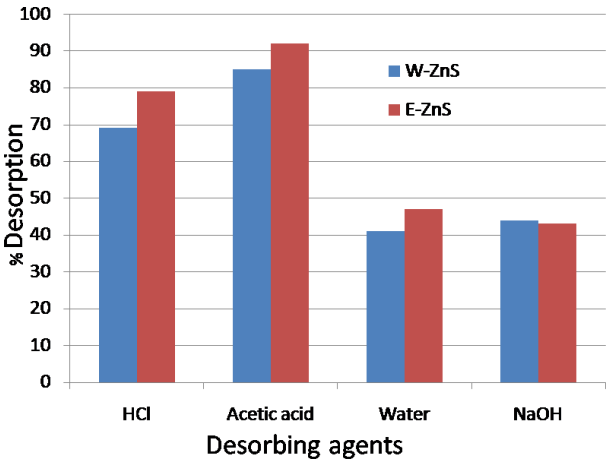

Fig. 8. Desorption of MB from W-ZnS and E-ZnS NPs from aqueous solution.

4. Conclusion

The study reports the surface modification of ZnS NPs with EDTA and WR extract and its application in removal of MB dye from aqueous solution. The surface functional groups, size and morphology of the W-ZnS and E-ZnS were assessed by FTIR, XRD and TEM techniques. The size of the E-ZnS NPs was found to be less than 10 nm, however, found to be agglomerated. The loading capacities of W-ZnS and E-ZnS NPs are found to be higher than many other adsorbents reported in literature. The loading capacity of E-ZnS was found to be high compared with W-ZnS NPs due to availability of more number of acidic sites on the surface. The removal of MB ions follow pseudo-second order kinetic model with monolayer adsorption process. The thermodynamic studies suggest that the present process is spontaneous and exothermic in nature suggesting that W-ZnS and E-ZnS NPs are superior adsorbents for the removal of MB from aqueous solution.

References

[1] A. Bhatnagar, M. Sillanpaa, Utilization of agro-industrial and municipal waste materials as potential adsorbents for water treatment—a review, Chem. Eng. J., 157 (2010) 277–296.

[2] N.A. Reddy, R. Lakshmipathy, N.C. Sarada, Application of *Citrullus lanatus* rind as biosorbent for removal of trivalent chromium from aqueous solution, Alexandria Eng. J., 53 (2014) 969–975.

[3] D. Mohan, C.U. Pittman, Activated carbons and low cost adsorbents for remediation of tri- and hexavalent chromium from water, J. Hazard. Mater., B137 (2006) 762–811.

[4] C. Wang, J. Li, X. Sun, L. Wang, X. Sun, Evaluation of zeolites synthesized from fly ash as potential adsorbents for wastewater containing heavy metals, J. Environ. Sci., 21 (2009) 127–136.

[5] R. Lakshmipathy, N.C. Sarada, A fixed bed column study for the removal of Pb^{2+} ions by watermelon rind, Environ. Sci. Water Res. Technol., 1 (2015) 244–250.

[6] R. Lakshmipathy, N.C. Sarada, Metal ion free watermelon (*Citrullus lanatus*) rind as adsorbent for the removal of lead and copper ions from aqueous solution, Desal. Wat. Treat., 57 (2016) 15362–15372.

[7] R. Jayachandra, R. Lakshmipathy, S.R. Reddy, Hydrophobic D-galactose based ionic liquid for the sequestration of Pb^{2+} ions from aqueous solution, J. Mol. Liq., 219 (2016) 1172–1178.

[8] T. Sheela, Y.A. Nayaka, R. Viswanatha, S. Basavanna, T.G. Venkatesha, Kinetics and thermodynamics studies on the adsorption of Zn(II), Cd(II) and Hg(II) from aqueous solution using zinc oxide nanoparticles, Powder Technol., 217 (2012) 163–170.

[9] A. Henglein, Small-particle research – physicochemical properties of extremely small colloidal metal and semiconductor particles, Chem. Rev., 89 (1989) 1861–1873.

[10] M. Hua, S. Zhang, B. Pan, W. Zhang, L. Lv, Q. Zhang, Heavy metal removal from water/wastewater by nanosized metal oxides: a review, J. Hazard. Mater., 211–212 (2012) 317–331.

[11] M. Khalkhali, Q. Liu, H. Zeng, H. Zhang, A size-dependent structural evolution of ZnS nanoparticles, Sci. Rep., 5 (2015) 14267.

[12] R. Chauhan, A. Kumar, R.P. Chaudhary, Photocatalytic degradation of methylene blue with Cu doped ZnS nanoparticles, J. Lumin., 145 (2014) 6–12.

[13] Y. Feng, N. Feng, G. Zhang, G. Du, One-pot hydrothermal synthesis of ZnS–reduced graphene oxide composites with enhanced photocatalytic properties, CrystEngComm, 16 (2014) 214–222.

[14] K. Ahmadi, M. Ghaedi, A. Ansari, Comparison of nickel doped Zinc Sulfide and/or palladium nanoparticles loaded on activated carbon as efficient adsorbents for kinetic and equilibrium study of removal of Congo Red dye, Spectrochim. Acta Part A, 136 (2015) 1441–1449.

[15] R. Lakshmipathy, K.M. Kumar, N.R. Anvesh, G. Srinivas, K.C. Mohan, L.M. Gomez, N.C. Sarada, ZnS nanoparticles capped with watermelon rind extract and their potential application in dye degradation, Res. Chem. Intermed., 43 (2017) 1329–1339.

[16] A. Srinivasan, T. Viraraghavan, Decolorization of dye wastewaters by biosorbents: a review, J. Environ. Manage., 91 (2010) 1915–1929.

[17] A. Mittal, V. Thakur, V. Gajbe, Adsorptive removal of toxic azo dye Amido Black 10B by hen feather, Environ. Sci. Pollut. Res., 20 (2013) 260–269.

[18] A. Saeed, M. Sharif, M. Iqbal, Application potential of grapefruit peel as dye sorbent: kinetics, equilibrium and mechanism of crystal violet adsorption, J. Hazard. Mater., 179 (2010) 564–572.

[19] A. Asfaram, M. Ghaedi, S. Hajati, M. Rezaeinejad, A. Goudarzi, M.K. Purkait, Rapid removal of Auramine-O and Methylene blue by ZnS:Cu nanoparticles loaded on activated carbon: a response surface methodology approach, J. Taiwan Inst. Chem. Eng., 53 (2015) 80–91.

[20] M. Ghaedi, Sh. Heidarpour, S.N. Kokhdan, R. Sahraie, A. Daneshfar, B. Brazesh, Comparison of silver and palladium nanoparticles loaded on activated carbon for efficient removal of Methylene blue: kinetic and isotherm study of removal process, Powder Technol., 228 (2012) 18–25,

[21] Y. Li, Q. Du, T. Liu, J. Sun, Y. Wang, S. Wu, Z. Wang, Y. Xia, L. Xia, Methylene blue adsorption on graphene oxide/calcium alginate composites, Carbohydr. Polym., 95 (2013) 501–507.

[22] M. Ghaedi, H.A. Larki, S.N. Kokhdan, F. Marahel, R. Sahraei, A. Daneshfar, M.K. Purkait, Synthesis and characterization of zinc sulfide nanoparticles loaded on activated carbon for the removal of methylene blue, Environ. Prog. Sustain. Energy, 32 (2013) 535–542.

[23] Y. Yao, S. Miao, S. Yu, L.P. Ma, H. Sun, S. Wang, Fabrication of Fe_3O_4/SiO_2 core/shell nanoparticles attached to graphene oxide and its use as an adsorbent, J. Colloid Interface Sci., 379 (2012) 20–26,

[24] G. Annadurai, R.S. Juang, D.J. Lee, Use of cellulose-based wastes for adsorption of dyes from aqueous solutions, J. Hazard. Mater., 92 (2002) 263–274.

[25] L. Mouni, L. Belkhiri, J. Bollinger, A. Bouzaza, A. Assadi, A. Tirri, F. Dahmoune, K. Madani, H. Remini, Removal of Methylene Blue from aqueous solutions by adsorption on Kaolin: kinetic and equilibrium studies, Appl. Clay Sci., 153 (2018) 38–45.

[26] J. Zhang, Y. Zhou, M. Jiang, J. Li, J. Sheng, Removal of methylene blue from aqueous solution by adsorption on pyrophyllite, J. Mol. Liq., 209 (2015) 267–271.

Supplementary data

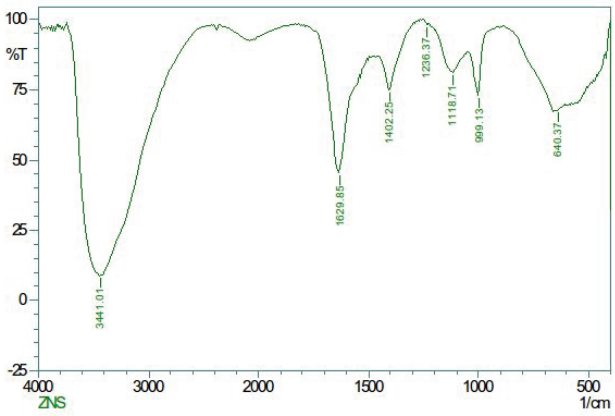

Fig. S1. FTIR spectra of unmodified ZnS NPs.

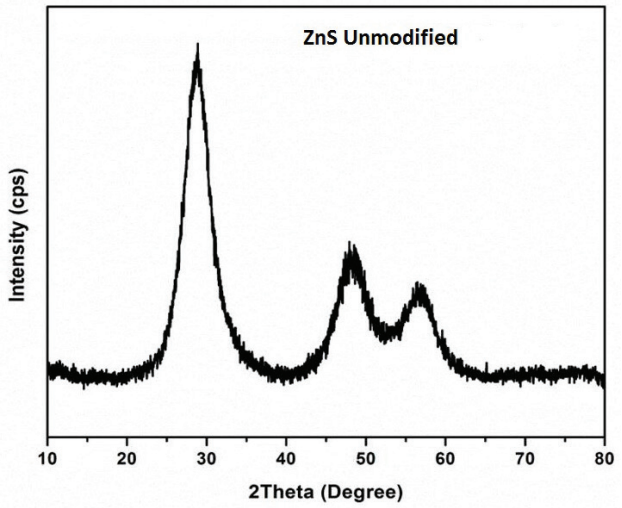

Fig. S2. XRD pattern of unmodified ZnS NPs.

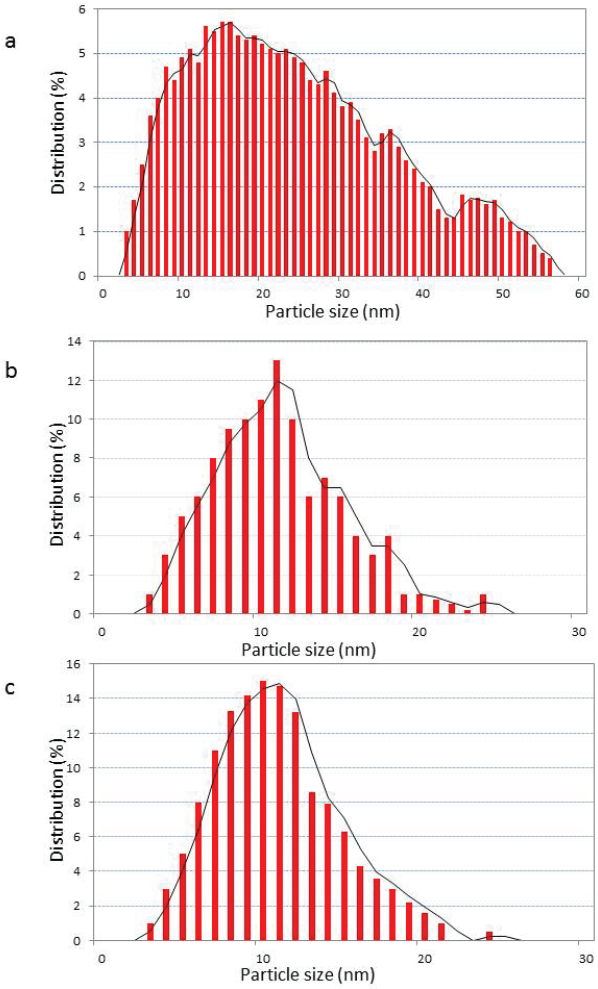

Fig. S3. Particle size distribution of (a) ZnS, (b) W-ZnS and (c) E-ZnS NPs.